



## Research paper

# Two dinuclear oxidovanadium(V) complexes of N<sub>2</sub>O<sub>2</sub> donor amine-*bis* (phenolate) ligands with bromo-peroxidase activities: Kinetic, catalytic and computational studies

Mainak Debnath<sup>a</sup>, Malay Dolai<sup>a</sup>, Kaberi Pal<sup>a</sup>, Arpan Dutta<sup>a</sup>, Hon Man Lee<sup>b</sup>, Mohammad Ali<sup>a,\*</sup>

<sup>a</sup> Department of Chemistry, Jadavpur University, 188, Raja Subodh Chandra Mullick Rd, Kolkata, West Bengal 700032, India

<sup>b</sup> Department of Chemistry, National Changhua University of Education, Changhua 50058, Taiwan

## ARTICLE INFO

## Article history:

Received 29 November 2017

Received in revised form 26 March 2018

Accepted 22 April 2018

## Keywords:

Oxido-bridged dinuclear vanadium(V) complexes

Crystal structures

Bromoperoxidase activities

Kinetic and catalytic studies.

DFT calculations

## ABSTRACT

Two dinuclear oxidovanadium(V) complexes [L<sup>i</sup>V<sup>VO</sup>(μ<sub>2</sub>-O)V<sup>VO</sup>(L<sup>i</sup>)] (i = 1, H<sub>2</sub>L<sup>1</sup>, complex **1** and i = 2 for H<sub>2</sub>L<sup>2</sup>, complex **2**) of two ONNO donor amine-*bis*(phenolate) ligands have been synthesized and characterized by X-ray diffraction studies which exhibited distorted octahedral geometry around each V center. In MeCN the complexes exist as dimers as indicated by HRMS studies, however, in the presence of 2 or more equivalents of H<sup>+</sup> the dimers turned into monomers, ([L<sup>i</sup>V<sup>VO</sup> = O])<sup>+</sup> which exists in equilibrium with ([L<sup>i</sup>V<sup>VO</sup> = OH])<sup>2+</sup> and evidenced from the shift in λ<sub>max</sub> from 685 nm to 765 nm for complex **1** and 600 to 765 nm for complex **2**. The complexes **1** and **2** efficiently catalyze the oxidative bromination of salicylaldehyde in the presence of H<sub>2</sub>O<sub>2</sub> to produce 5-bromo-salicylaldehyde as the major product with TONs 405 and 450, respectively in the mixed solvent system (H<sub>2</sub>O:MeOH:THF = 4:3:2, v/v). The kinetic analysis of the bromide ion oxidation reaction indicates a mechanism which is first order in peroxidovanadium complex and bromide ion and limiting first-order on [H<sup>+</sup>]. The evaluated k<sup>Br</sup> and k<sup>H</sup> values are (8.82 ± 0.35) and (65.0 ± 2.23) M<sup>-1</sup> s<sup>-1</sup> for complex **1** and (6.74 ± 0.19) and (61.87 ± 2.27) M<sup>-1</sup> s<sup>-1</sup> for complex **2**, respectively. The K<sub>a</sub> of protonated species ([L<sup>i</sup>V<sup>VO</sup> = OH])<sup>2+</sup> are: K<sub>a</sub> = (4.3 ± 0.40) × 10<sup>-3</sup> (pK<sub>a</sub> = 2.37) and (4.7 ± 0.50) × 10<sup>-3</sup> (pK<sub>a</sub> = 2.33) for complex **1** and **2** respectively. On the basis of the chemistry displayed by these model compounds, a mechanism of bromide oxidation and a tentative catalytic cycle have been framed which might be relevant to vanadium haloperoxidase enzymes and supported by DFT calculations.

© 2018 Elsevier B.V. All rights reserved.

## 1. Introduction

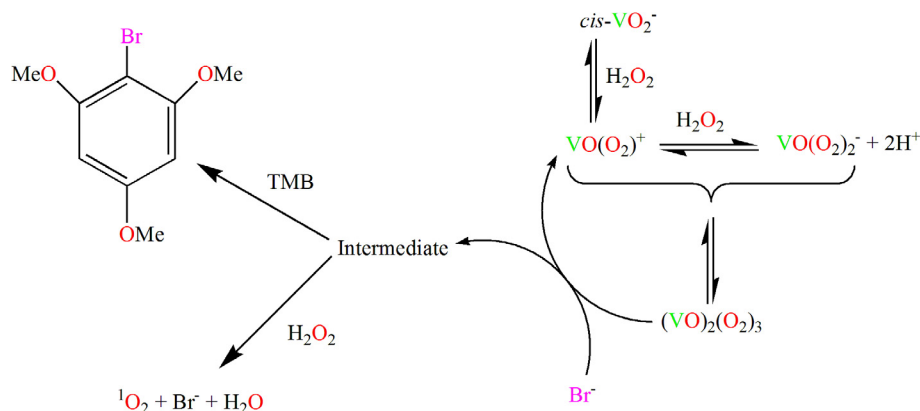
Structural and functional modeling of biological activities of various vanadium containing enzymes have long been of interest to chemists. The discovery of the presence of vanadium(V) in the active site of vanadium dependent haloperoxidases (V-HalPO) [1] and its importance in catalytic reactions [2–9] has stimulated the research on coordination chemistry of vanadium. Haloperoxidases are the enzymes that catalyze the oxidation of halides to the corresponding hypohalous acids or to a related two-electron oxidized halogenating intermediate such as OX<sup>-</sup>, X<sub>3</sub><sup>-</sup> and X<sup>+</sup> in the presence of H<sub>2</sub>O<sub>2</sub> as oxidant which in the subsequent step reacts with suitable nucleophilic acceptors to form the corresponding halogenated compounds [10–14]. Kinetic studies suggest the formation of peroxido-vanadium intermediate, which ultimately facilitates the

halogenation of various organic substrates possibly via the reaction of HOX, X<sub>2</sub> or X<sub>3</sub> [12–14]. In the case of bromoperoxidase, the existence of peroxido as well as hypobromite-like vanadium intermediates in solution have been demonstrated [15,16]. Besides, evidence for peroxide binding to the active center of bromoperoxidase isolated from *Ascophyllum nodosum* has been presented by Čásný et al. [17].

To get a better understanding of the working mechanism of the vanadium haloperoxidase enzyme and to determine the role of vanadium, a variety of vanadium compounds have been studied as functional models [12]. The first reported functional mimic of V-BrPO is *cis*-dioxido vanadium(V) [V(O<sub>2</sub>)<sub>2</sub>]<sup>+</sup> in acidic aqueous solution [18,19]. *cis*-Dioxido-vanadium(V) catalyze the bromination of 1,3,5-trimethoxybenzene (TMB) and also the bromide-mediated disproportionation of H<sub>2</sub>O<sub>2</sub>. In a first step, H<sub>2</sub>O<sub>2</sub> is complexed to give red oxidoperoxido [VO(O<sub>2</sub>)<sub>2</sub>]<sup>+</sup> and yellow oxidodiperoxido [VO(O<sub>2</sub>)<sub>2</sub>]<sup>-</sup> complexes, the ratio between them depends on the H<sub>2</sub>O<sub>2</sub> concentration and the pH of the medium. In a second step

\* Corresponding author.

E-mail address: [mali@chemistry.jdvu.ac.in](mailto:mali@chemistry.jdvu.ac.in) (M. Ali).



**Scheme 1.** Bromination activity of the V-BrPO mimic *cis*-dioxidovanadium(V) [18]

these two species combine to give dioxidotriperoxido-divanadium(V) [(VO)<sub>2</sub>(O<sub>2</sub>)<sub>3</sub>] compound, which is considered to be the actual oxidant (Scheme 1).

Contrary to the natural haloperoxidases, *cis*-dioxidovanadium(V) functions only at low pH (2 or less), because at lower acidity the amount of monoperoxidovanadate is insufficient for dimerisation to form [(VO)<sub>2</sub>(O<sub>2</sub>)<sub>3</sub>].

Another difference with the enzyme is its low catalytic rate indicating the importance of the presence of protein environment around the active site. A V-BrPO mimic that has been well studied is the oxidovanadium(V) complex of hydroxyphenylsalicylideneamine [(HPS)VO(OEt)(EtOH)] [20]. The bromination reaction becomes catalytic when acid is used in at least stoichiometric quantities with respect to H<sub>2</sub>O<sub>2</sub>. Nevertheless, the exact nature of this halogenating intermediate has not been determined as yet.

The structure of vanadium haloperoxidase contains the vanadium ion attached to the protein backbone via one histidine nitrogen donor atom, whilst the oxido moieties are strongly H-bonded to arginine, lysine, histidine and serine amino acids [20] (Fig. 1).

In the view of the above observations, we have decided to design and synthesize structural and functional models of the biomolecules, which has the potential ability to catalyze the bromination of organic substrate in order to get a better understanding of the mechanism of such reactions. Meanwhile, we have been interested in vanadium chemistry of amine *bis*-phenolate ligands showing interesting catalytic activities towards hydrocarbon oxidation and epoxidation reactions [21–24]. We will reveal here the structures of two oxido-bridged dinuclear vanadium complexes of N<sub>2</sub>O<sub>2</sub> donor amine-*bis*(phenolate) ligands (Scheme 2) that showed interesting bromoperoxidase activity towards the bromination of salicylaldehyde.

## 2. Experimental

### 2.1. Physical measurements

Perkin-Elmer 240 elemental analyzer was used for elemental analyses while IR (Infrared) spectra were recorded from KBr pellets on a Nicolet Magna IR 750 series-II FTIR spectrophotometer in the range 400–4000 cm<sup>-1</sup>. Agilent 8453 UV-Vis diode-array spectrophotometer was used to record the electronic spectra. Mass spectra were recorded on an HRMS (model XEVO G2QTof) spectrometer. Electrochemical measurements were carried out using a computer controlled AUTOLAB (Model: AutoLab 302) cyclic voltammeter with platinum working electrode, platinum-wire counter electrode and saturated calomel (SCE) reference electrode in MeCN using tetrabutylammonium perchlorate as supporting electrolyte.

### 2.2. Materials

Starting materials for the synthesis of the ligands (H<sub>2</sub>L<sup>1</sup> and H<sub>2</sub>L<sup>2</sup>) and their vanadium(V) complexes (1 and 2), namely, 2, 4-di-*tert*-butylphenol (Aldrich), 2-aminoethylpyridine (Aldrich), N, N'-dimethyl-ethylenediamine (Aldrich), formaldehyde (Merck India), [VO(acac)<sub>2</sub>] (Lancestar India), are of reagent grade and used as received. Substrates namely salicylaldehyde (Aldrich) used in the catalytic reactions is of reagent grade and used as received. 30% H<sub>2</sub>O<sub>2</sub> (Merck India), KBr (Merck India) and 70% of HClO<sub>4</sub> were used in the catalytic bromination reactions.

### 2.3. Synthesis of amine-*bis*(phenolate) ligand

The ligands (H<sub>2</sub>L<sup>1</sup> and H<sub>2</sub>L<sup>2</sup>) have been synthesized according to a reported method [25] and further characterized by CHN and <sup>1</sup>H NMR analyses.

H<sub>2</sub>L<sup>1</sup>: Yield 83%. *Ana. Cal* value for Molecular formula, C<sub>37</sub>H<sub>54</sub>N<sub>2</sub>O<sub>2</sub> C, 79.52%; H, 9.74%; N, 5.01%; *Found* C, 79.16%; H 9.52%; N, 5.15%. <sup>1</sup>H NMR (δ, ppm) 1.28 (s, 36-H); 2.81 (t, 2-H); 3.10 (t, 2-H); 3.73 (s, 4-H); 6.87–7.22 (m, 6-ArH); 7.57 (t, 1-ArH); 8.688 (d, 1-ArH); 9.45 (b, -OH protons) (Fig. S1).

H<sub>2</sub>L<sup>2</sup>: Yield 89%. *Ana. Cal* value for Molecular formula, C<sub>34</sub>H<sub>56</sub>N<sub>2</sub>O<sub>2</sub> C, 74.12%; H, 9.05%; N, 7.86%; *Found* C, 73.56%; H 9.01%; N, 7.25%. <sup>1</sup>H NMR (δ, ppm) 2.18 (s, 6-H); 2.25 (s, 12-H); 2.63 (s, 4-H); 3.65 (s, 4-H); 6.79 (s, 2-ArH); 7.20 (s, 2-ArH); 9.36 (s, -OH protons) (Fig. S2).

### 2.4. Preparation of complexes

#### 2.4.1. Synthesis of [VO(L<sup>1</sup>)<sub>2</sub>O] (1)

1.0 mmol (0.558 g) of the ligand H<sub>2</sub>L<sup>1</sup> was dissolved in 20 ml MeCN and was refluxed with 2 mmol (0.202 g) TEA for 10 min. The solution was then cooled and a solution of [VO(acac)<sub>2</sub>] (1 mmol, 0.265 g) in MeCN was added dropwise to it and refluxed for 3 h. The resulting dark blue solution was filtered off after cooling to room temperature and the filtrate was subjected to slow evaporation at room temperature, whereupon dark blue block shaped single crystals suitable for X-ray study were obtained within 3 days.

[VO(L<sup>1</sup>)<sub>2</sub>O]: Yield 70%. *Ana. Cal* value for Molecular formula, C<sub>74</sub>H<sub>104</sub>N<sub>4</sub>O<sub>7</sub>V<sub>2</sub> C, 70.34%; H, 8.30%; N, 4.43%; *Found* C, 70.12%; H, 8.19%; N, 4.36%. FTIR (KBr disc; cm<sup>-1</sup>) ν(V=O) 934 and ν(V-O-V) 757 (Fig. S3). <sup>1</sup>H NMR (δ, ppm) 1.19–1.44 (m, 72-H); 2.50 (s, 4-H); 2.79 (s, 4-H); 3.22 (d, 4-H); 3.73 (s, 4-H); 6.01 (d, 2-ArH); 6.67–7.34 (m, 14-ArH) (Fig. S4).

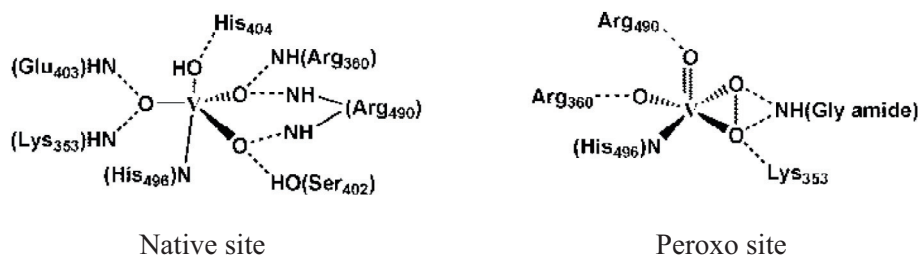
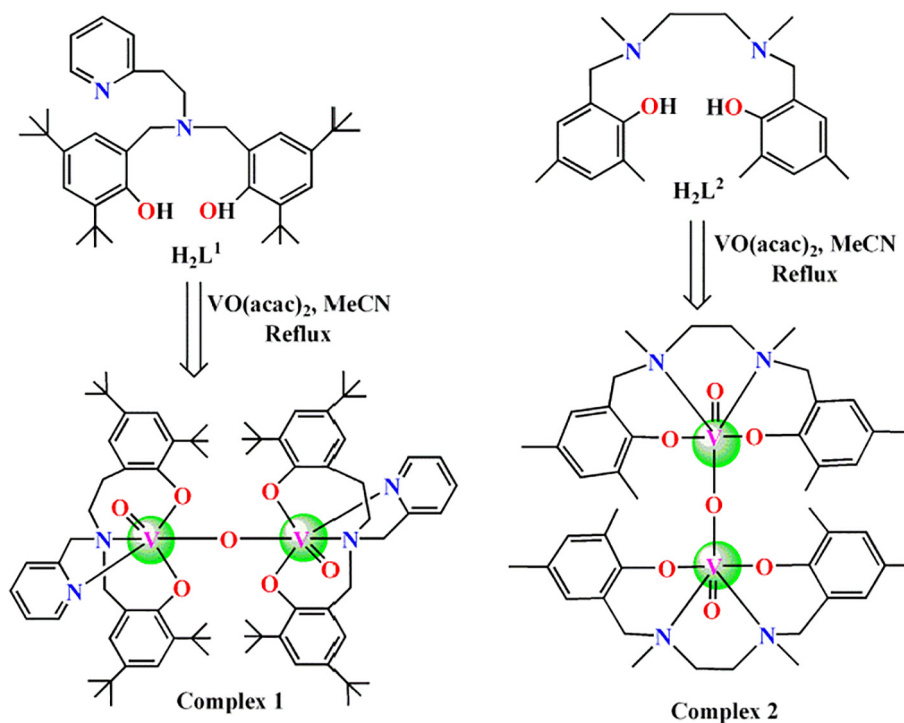


Fig. 1. The native and peroxidovanadium site in V-CPOs [20].



Scheme 2. Schematic presentation of preparation of the complexes **1** and **2** from ligands  $H_2L^1$  and  $H_2L^2$  respectively.

#### 2.4.2. Synthesis of $[VO(L^2)]_2O$ (**2**)

Complex **2** was synthesized following the same procedure as in complex **1** taking  $H_2L^2$  ligand instead of  $H_2L^1$ .

$[VO(L^2)]_2O$ : Yield 70%. *Ana. Cal* value for Molecular formula,  $C_{44}H_{60}N_4O_7V_2$ , C, 61.40%; H, 7.06%; N, 7.78%; *Found* C, 61.29%; H, 6.95%; N, 7.62%. FTIR (KBr disc;  $cm^{-1}$ )  $\nu(V=O)$  939 and  $\nu(V-O-V)$  776.  $^1H$  NMR ( $\delta$ , ppm) 2.20 (s, 8-H); 2.25 (s, 12-H); 2.54–2.91 (m, 24-H); 3.09 (t, 4-H); 3.58 (d, 4-H); 6.18 (s, 2-ArH); 6.60 (s, 2-ArH); 6.68 (s, 2-ArH); 6.89 (s, 2-ArH) (Fig. S5).

#### 2.5. X-Ray crystallography

Intensity data of the complexes **1** and **2** were collected on a smart CCD diffractometer at 150(2) K in the  $\omega$ - $2\theta$  scan mode in the range  $2.75 < 2\theta < 27.50^\circ$ . The intensities were corrected for Lorentz and polarization effects and for absorption using the  $\psi$ -scan method. The diffraction data for complex **2** were collected with a KM4 CCD diffractometer with a four-circle area-detector (KUMA Diffraction, Poland) equipped with an Oxford Cryostream Cooler (Oxford Cryosystems, UK).  $MoK_\alpha$  radiation ( $\lambda = 0.71073 \text{ \AA}$ ) (monochromator Enhance, Oxford Diffraction, UK) was used in all measurements. The cell parameters were refined from all strong reflections. The data reductions were carried out using the CrysAlis RED (Oxford Diffraction, UK) program. Both the structures were

determined by direct methods using SHELXS-97 [26] and refined anisotropically on  $F^2$  using the full-matrix least-squares procedure of SHELXL-97 [27]. The data for publication were prepared by SHELXL and PARST [28]. The crystal data collection and the procedure for data refinement are listed in Table 1 for the two complexes.

#### 2.6. Experimental set up for catalytic bromination

In this method, a representative substrate, namely salicylaldehyde (20 mmol), was dissolved in mixed solvent ( $H_2O:MeOH:THF = 4:3:2$ ) [29] and the resulting solution was taken in a 50 ml capacity round bottom flask. To the above solution was then added KBr (40 mmol) followed by 2 ml (67 mmol) of 30%  $H_2O_2$ .

An appropriate catalyst (say, complex **1**) (0.05 g, 0.04 mmol) and 70%  $HClO_4$  (0.10 ml) were added to it and the reaction was initiated with stirring. After 2 h of stirring at ambient temperature 0.1 ml of 70%  $HClO_4$  was further added and stirring was continued for next 10 h. The separated white product was filtered, washed with water followed by diethyl ether and dried in air. The crude mass was dissolved in  $CH_2Cl_2$  and insoluble material was separated by filtration. After evaporation of the solvent to ca. 5 ml it was loaded over column packed with silica gel. The fast moving band on elution with  $CH_2Cl_2$  was collected and evaporated to dryness

**Table 1**  
Crystal data and structure refinement parameter of the complexes **1** and **2**.

	Complex <b>1</b> (CCDC 1454101)	Complex <b>2</b> (CCDC 853756)
Formula	C <sub>74</sub> H <sub>104</sub> N <sub>4</sub> O <sub>7</sub> V <sub>2</sub>	C <sub>44</sub> H <sub>60</sub> N <sub>4</sub> O <sub>7</sub> V <sub>2</sub> , C <sub>2</sub> H <sub>3</sub> N
Formula Weight	1263.49	899.89
Crystal System	Triclinic	Monoclinic
Space group	<i>P</i> -1 (No. 2)	<i>P</i> 2 <sub>1</sub> /c
<i>a</i>	10.5200(9)	10.573(5)
<i>b</i> [Å]	15.7749(13)	16.368(5)
<i>c</i>	22.8117(19)	25.925(5)
$\alpha$	79.824(1)	90
$\beta$ [°]	85.973(2)	95.188(5)
$\gamma$	75.321(1)	90
<i>V</i> [Å <sup>3</sup> ]	3603.2(5)	4468(3)
<i>Z</i>	2	4
<i>D</i> (calc) [g/cm <sup>3</sup> ]	1.165	1.338
$\mu$ (MoK $\alpha$ ) [1/mm]	0.312	0.474
<i>F</i> (0 0 0)	1356	1904.0
Crystal Size [mm]	0.20 × 0.20 × 0.25	0.04 × 0.04 × 0.06
Temperature (K)	150	150
Radiation [Å]	0.71073	0.71073
$\theta$ Min-Max [°]	2.2, 28.7	2.30, 26.0
Dataset	−14; 14; −21; 21;	−13; 13; −20; 20;
	−30; 30	−31; 31
Tot., Uniq. Data, <i>R</i> (int)	52901, 18724, 0.140	23769, 8721, 0.160
Observed data [1 greater than 2.0 $\sigma$ ( <i>I</i> )]	6690	5281
<i>N</i> <sub>ref.</sub> , <i>N</i> <sub>par</sub>	18724, 787	8721, 542
<i>R</i> , <i>wR</i> <sub>2</sub> , <i>S</i>	0.0905, 0.2935, 1.03	0.1017, 0.2716, 1.047

to give 5-bromo-salicylaldehyde. We have performed the several sets of such reaction for varying time (3h, 6 h, 9 h and 12 h) and products were isolated and quantified in each case. Then the calculated yield (%) are tabulated in Table 3.

### 2.7. DFT calculations

The ground state optimized structures of free complex **2** and its probable catalytic intermediates formed during oxidative bromination of salicylaldehyde have been carried out using DFT [30] method in a Gaussian 09 W software package [31]. Becke's hybrid function [32] along with the Lee-Yang-Parr (LYP) correlation function [33] were used throughout the study. The geometry of all the structures were fully optimized without any symmetry constraints. LanL2dz basis set under B3LYP was used for all the atoms during the optimization of ground state geometries.

## 3. Results and discussion

### 3.1. Syntheses

Tetradentate H<sub>2</sub>L<sup>i</sup> (*i* = 1 or 2) ligands were synthesized by simple Mannich condensation of 2-amino-ethylpyridine with 2,4-ditertiarybutylphenol and *N,N'*-dimethyl-ethylenediamine with 2,4-dimethylphenol in the presence of formaldehyde in MeOH. Straight forward reactions between equimolar amounts of each of the ligands and [VO(acac)<sub>2</sub>] and two equivalents of TEA in MeCN separately under reflux afford complexes **1** and **2**.

### 3.2. Structural descriptions of [VO(L<sup>1</sup>)<sub>2</sub>O] (**1**) and [VO(L<sup>2</sup>)<sub>2</sub>O] (**2**)

The molecular structures of complexes **1** and **2** are depicted in Fig. 2 and Fig. 3 respectively. Some selected bond distances and bond angles are summarized in Table 2 and Table S1, respectively for complexes **1** and **2**.

Complex **1** crystallizes in the triclinic system of space group *P*-1 while complex **2** crystallizes in the monoclinic system with space group *P*2<sub>1</sub>/c. In Complex **1** the asymmetric unit contains two crystallographically independent dinuclear units A and B which are isostructural but slightly different with respect to their respective bond distances and bond angles and are bridged by O6 and O2 respectively. In complex **2** the two vanadium centers are bridged by O2. It is interesting to note that in both asymmetric unit A and B of complex **1**, co-linear oxido atom exactly bisects the two metal centres (V1-O6 = 1.792 Å and V2-O2 = 1.7945 and lie in the expected region [34] but this is closely missed in complex **2** (O2-V2 = 1.796 Å and O2-V1 = 1.782 Å). In complex **1** the relative disposition of the two V=O groups are exactly *trans*, with O5 = V1...V1#1 = O5#1 torsion angle of 180°, whereas, in complex **2**, the relative disposition of the two V=O groups is somewhat twisted with O3 = V1...O1 = V2 torsion angle of 133.33°.

The two vanadium centres in asymmetric units A and B of complex **1** are in distorted octahedral geometry with O7-V1-O8 and O4-V2-O1 bond angles of 161.38° and 163.82°, respectively indicating a significant deviation from the ideal value of 180°. Similarly, in complex **2**, O5-V1-O6 (163.14°) and O7-V2-O8 (161.7°) angles are also significantly deviated from 180°. In asymmetric unit A of complex **1** the axial positions are held by donor atoms like N2 and O5 (terminal). The basal coordinates are taken up by donor atoms like N1, O7, O8 and O6 (bridging). In complex **2** the axial

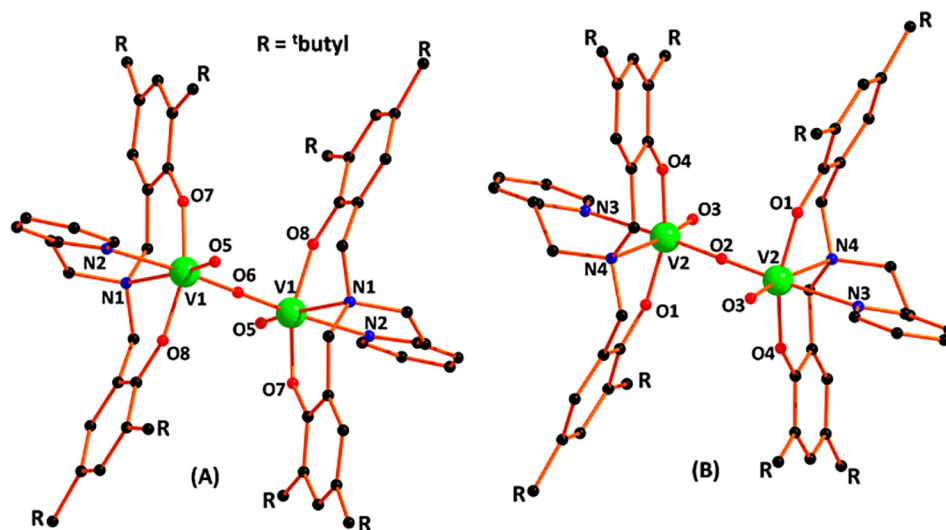


Fig. 2. Molecular view of complex **1**; H atoms are omitted for clarity.

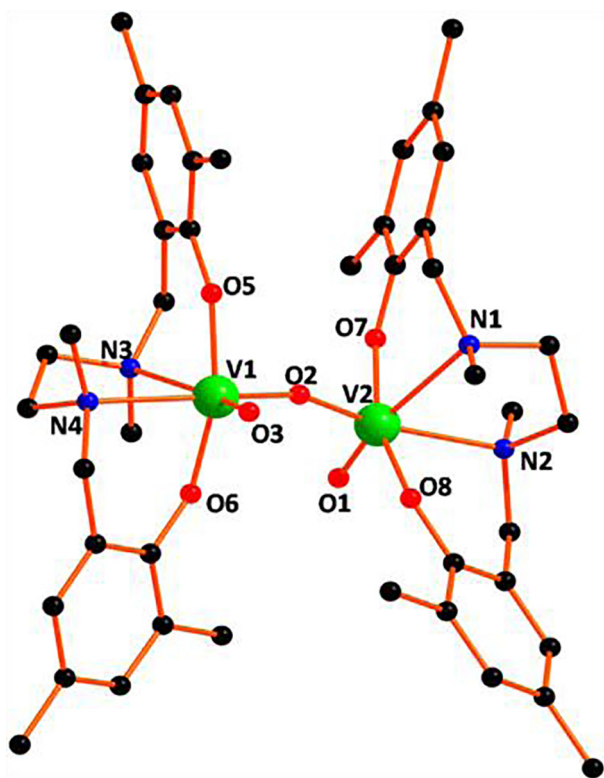


Fig. 3. Molecular view of complex **2**; H atoms are omitted for clarity.

**Table 2**  
Selected bond distances of complex **1** and **2**.

Complex 1		Complex 2	
N1-V1	2.329(5)	V1-O3	1.611(4)
N2-V1	2.387(4)	V1-O2	1.783(5)
N3-V2	2.320(5)	V1-O5	1.861(4)
N4-V2	2.392(4)	V1-O6	1.873(5)
O1-V2	1.844(4)	V1-N4	2.284(5)
O2-V2	1.7945(10)	V1-N3	2.399(5)
O3-V2	1.603(3)	V2-O1	1.597(4)
O4-V2	1.845(4)	V2-O2	1.795(5)
O5-V1	1.604(3)	V2-O7	1.875(5)
O6-V1	1.7918(8)	V2-O8	1.881(5)
O7-V1	1.840(3)	V2-N2	2.273(6)
O8-V1	1.851(3)	V2-N1	2.367(5)

positions are also taken up by N3 and O3 (terminal) for V1 and N1 and O1 (terminal) for V2 centre. The equatorial positions are occupied by donor atoms N4, O5, O6. O2 (bridging) for V1 while N2, O7, O8 and O2 (bridging) atoms for V2 centre.

In the asymmetric unit A of complex **1**, the central metal atom is shifted towards the terminal oxygen atom (O5) by 0.184 Å from the equatorial plane defined by N1, O7, O6 and O8. In case of complex **2** the V1 atom is shifted from the equatorial plane towards the terminal oxygen O3 by 0.257 Å whereas the V2 center is shifted by 0.263 Å.

The distances between the terminal oxygen atom and central metal atoms in both the complexes fall in the comparable range (V1-O5 = 1.603 Å for complex **1A** and V1-O3 = 1.611 and V2-O1 = 1.597 Å for complex **2**) with other structurally characterized oxido-vanadium complexes [35]. In both the complexes, the significant longer distances between the axial and equatorial nitrogen atom from the central vanadium atom (V1-N2 = 2.387 Å and V1-N1 = 2.329 Å for complex **1**; V1-N3 = 2.399 Å, V2-N1 = 2.367

Å, V1-N4 = 2.284 Å and V2-N2 = 2.274 Å for complex **2**) reveal the weakening of V-N bonds.

### 3.3. Electrochemical study

The electrochemical behavior of complex **2** (Fig. 4) was studied by cyclic voltammetry in the range +1.00 to -1.00 V at a scan rate 100 mVs<sup>-1</sup> in Acetonitrile at platinum electrode versus SCE using tetrabutyl-ammonium perchlorate (TBAPC) as supporting electrolyte. The complex **1** and **2** remain as dinuclear entities as evidenced from HRMS spectra (Figs. S6a and S6b). The two anodic peaks at -0.042 and 0.417 V correspond (peak to peak separation value is 0.459 V) to V(IV)-V(IV) → V(V)-V(IV) and V(V)-V(IV) → V(V)-V(V) oxidations while the cathodic peaks at 0.348 (not well resolved) and -0.141 V (peak to peak separation value is 0.489 V) correspond to V(V)-V(V) → V(IV)-V(V) and V(IV)-V(V) → V(IV)-V(IV) reductions. The  $E_{1/2} = 0.382$  V corresponds to V(IV)-V(V) = V(V)-V(V) process and  $E_{1/2} = -0.091$  V corresponds to V(IV)-V(IV) = V(IV)-V(V) process. The 1st redox couple (V(IV)-V(V)/V(V)-V(V)) appears to be quasi-reversible, whereas the other couple V(IV)-V(IV)/V(V)-V(IV) is found to be irreversible. Controlled coulometric experiment shows that the wave is one electron transfer process. As the phenolate ligand as well as methoxy group could not be reduced in this potential range [36], we assign them as metal centered reduction potentials for the VO<sup>3+</sup>/VO<sup>2+</sup> couple. No reproducible CV for complex **1** was obtained.

### 3.4. Electronic spectra

Absorption spectra of complex **1** shows one peak at 685 nm ( $\epsilon/M^{-1}cm^{-1} = 3040$ ) and a hump at 565 nm ( $\epsilon/M^{-1}cm^{-1} = 2640$ ) whereas complex **2** shows a peak at 600 nm ( $\epsilon/M^{-1}cm^{-1} = 3080$ ) which may be attributed to the ligand (Phenoxido) to metal [V(V)] charge transfer (LMCT) bands (Fig. S7).

### 3.5. Oxidative bromination of salicylaldehyde

Vanadium(V) complexes were found to catalyze the oxidative bromination of organic substrates in the presence of H<sub>2</sub>O<sub>2</sub> and bromide ion [37,38] where vanadium centers were claimed to be coordinated by 1 or 2 equivalents of H<sub>2</sub>O<sub>2</sub>, forming oxido-monoperoxido, [VO(O<sub>2</sub>)]<sup>+</sup> and oxido-diperoxido, [VO(O<sub>2</sub>)<sub>2</sub>]<sup>+</sup> species which ultimately gave rise to the actual oxidant [(VO)<sub>2</sub>(O<sub>2</sub>)<sub>3</sub>]

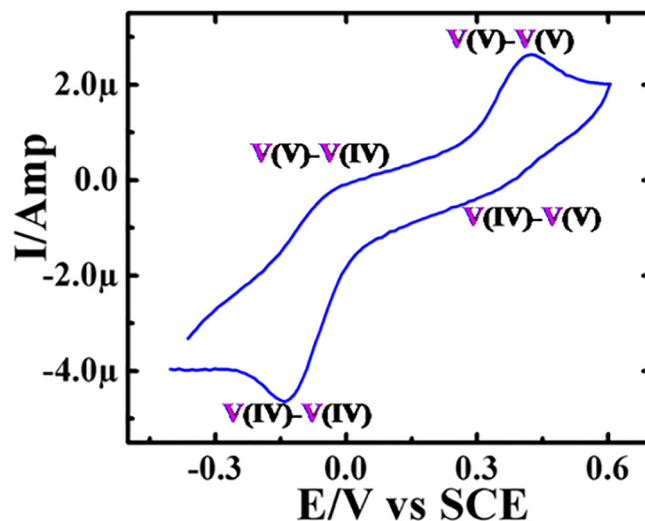
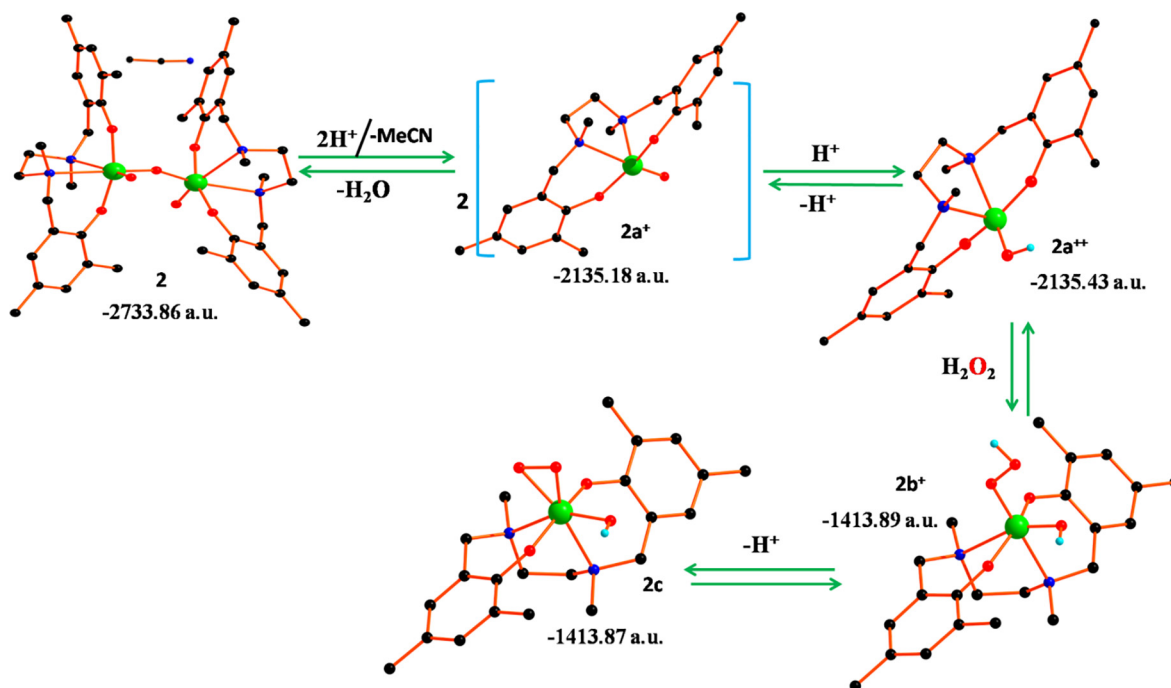


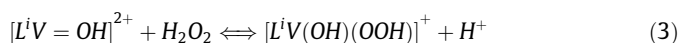
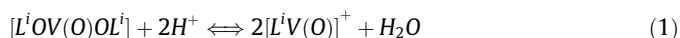
Fig. 4. CV of complex **2** in MeCN solvent at 25 °C, [C] = 1.0 mM; [TBAPC] = 0.10 M, scan rate = 100 mVs<sup>-1</sup>.



**Scheme 3.** Schematic presentation of the formation different intermediates of complex **2** in the presence of HClO<sub>4</sub> and H<sub>2</sub>O<sub>2</sub>.

[20,39] to oxidize bromide ion most likely to HOBr and brominates the substrates.

Here also complexes **1** and **2** are found to catalyze the bromination of salicylaldehyde in the presence of H<sub>2</sub>O<sub>2</sub> and bromide ion. In acidic medium both the dinuclear complexes [L<sup>i</sup>OV(O)VOL<sup>i</sup>] turn into mononuclear species [L<sup>2</sup>V = O]<sup>+</sup> (See the HRMS data in Sup file, Fig. S8) through the abstraction of bridging O atom by H<sup>+</sup> eliminating one water molecule (Scheme 3) which may be in equilibrium [L<sup>i</sup>V = O]<sup>+</sup> + H<sup>+</sup> ⇌ [L<sup>i</sup>V = OH]<sup>2+</sup> and reacts with H<sub>2</sub>O<sub>2</sub> to form hydroxido-hydroperoxido species, [L<sup>i</sup>V(OH)(OOH)]<sup>+</sup> and then hydroxido-peroxidospecies [L<sup>i</sup>V(OH)(O<sub>2</sub>)] (Eq. (13), Scheme 3) as the active intermediate for the catalytic oxidation of Br<sup>-</sup> to Br<sup>+</sup> and to brominate the substrate Scheme 4.



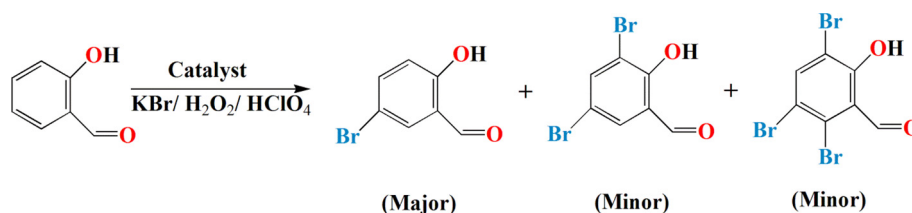
It is proposed that dioxidovanadium(V) [L<sup>2</sup>V(O)<sub>2</sub>]<sup>+</sup> (Scheme 5, see later), formed through the oxidation of Br<sup>-</sup> to Br<sup>+</sup> by [L<sup>2</sup>V(OH)(O<sub>2</sub>)] which is again formed from [L<sup>2</sup>V(OH)(OOH)]<sup>+</sup> (Scheme 3), satisfactorily catalyzes the oxidative bromination of salicylaldehyde to give 5-bromosalicylaldehyde as major product along with 3,5-dibromosalicylaldehyde and 2,3,5-tribromosalicylaldehyde as minor products (Fig. S9) using H<sub>2</sub>O<sub>2</sub>/KBr in the

presence of HClO<sub>4</sub> in mixed solvents (H<sub>2</sub>O:MeOH:THF = 4:3:2) [29] at room temp.; cf. Scheme 3. The presence of acid was found to be essential during the catalytic reaction to facilitate the bromination reaction, but an excess of HClO<sub>4</sub> (≥80 mmol) causes decomposition of the catalysts as well as lowering of selectivity of the reaction. In the absence of acid no catalysis were observed. Under the reaction conditions, a maximum of ~89% conversion was achieved with both the complexes (Table 3).

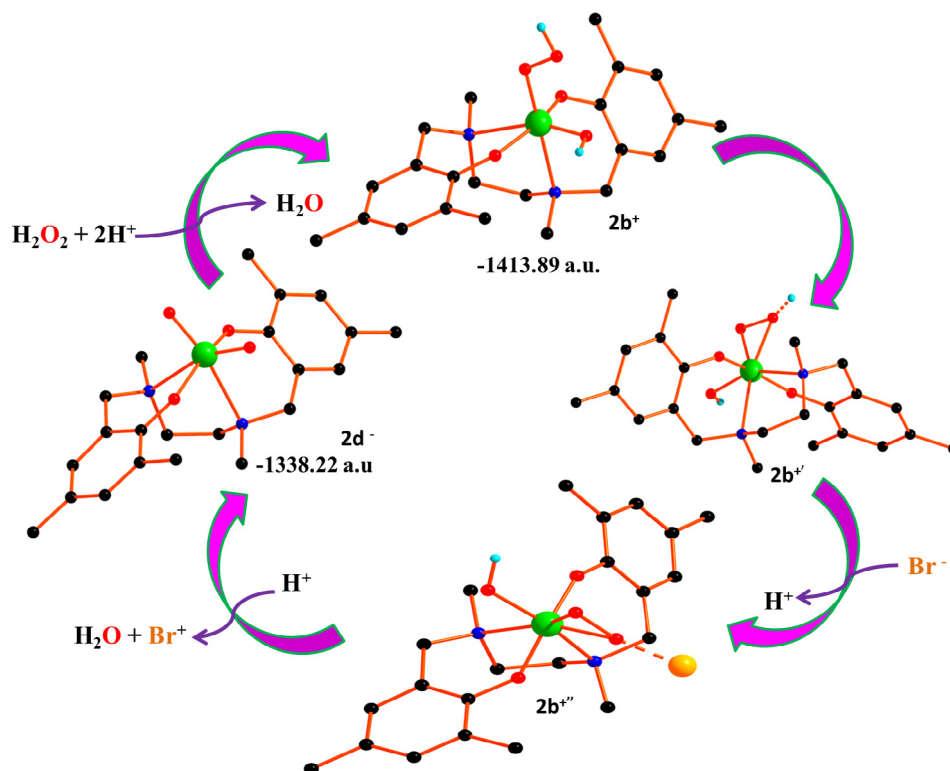
In the absence of catalyst, the reaction mixture gave only 4% conversion of salicylaldehyde to 5-bromosalicylaldehyde. Almost comparable conversion of the substrate, TON as well as selectivity were achieved for complexes **1** and **2**.

### 3.6. Kinetic and mechanistic studies

It was observed that complexes **1** and **2** ([L<sup>i</sup>OV(O)VOL<sup>i</sup>]) satisfactorily catalyze the oxidative bromination of salicylaldehyde to give 5-bromosalicylaldehyde in the presence of H<sub>2</sub>O<sub>2</sub>/KBr and HClO<sub>4</sub> in mixed solvents (H<sub>2</sub>O:MeOH:THF = 4:3:2) [29] at room temp. However, all the kinetic studies have been carried out in MeCN by following the change in absorbance at 685 nm (λ<sub>max</sub> for complex **1**) and 765 nm. Addition of 2 or more equivalents of HClO<sub>4</sub> to an acetonitrile solution of the complex **1** produced observable changes in the UV/visible spectra with a shift in λ<sub>max</sub> from 685 nm to 765 nm for complex **1**. Similarly λ<sub>max</sub> at 600 was shifted to 765 nm for complex **2**. The oxidation of Br<sup>-</sup> to Br<sup>+</sup> by the reaction with [L<sup>i</sup>V(OH)(OOH)]<sup>+</sup> is given in Eq. (4) (i = 1 or 2



**Scheme 4.** Catalytic reaction products.



**Scheme 5.** Proposed catalytic cycle for the oxidative bromination of salicylaldehyde catalyzed by complex **2**.

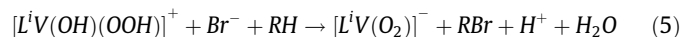
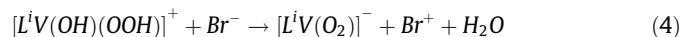
**Table 3**

Catalytic parameters for the bromination of salicylaldehyde by KBr/H<sub>2</sub>O<sub>2</sub> (KBr = 40 mmol, H<sub>2</sub>O<sub>2</sub> = 2 ml i.e. 67 mmol) using complexes **1** and **2** as catalysts (0.04 mmol) in mixed solvents H<sub>2</sub>O:MeOH:THF = 4:3:2 [29] at room temperature (25 °C) in presence of 0.2 ml HClO<sub>4</sub>.

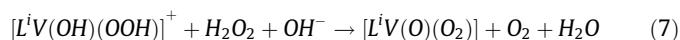
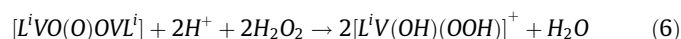
Catalyst	Substrate (mmol)	Reaction time (hr)	Conversion (%)	% Yield		Selectivity	TON <sup>†</sup>
				5-Br-sal (major)	3,5-di-Br-sal (minor)		
Complex <b>1</b>	20	3	12	10	2	83.3	445
		6	37	33	4	89.1	
		9	66	58	8	87.8	
		12	89	74	15	83	
Complex <b>2</b>	20	3	12	9	3	75.0	440
		6	40	31	9	77.5	
		9	67	52	15	77.6	
		12	88	70	18	79.5	

<sup>†</sup> TON is determined by the ratio of No. of moles of substrate converted to product and the number of moles of catalyst (0.04 mmol) used.

for complexes **1** and **2** respectively). The product observed by UV/visible spectroscopy is primarily tribromide under the experimental conditions used here but without substrate (RH). In the presence of an organic substrate capable of electrophilic aromatic substitution, reaction (5) leads to halogenations.



However, in the absence of an organic substrate, dioxygen gas was generated upon the addition of an equivalent of hydrogen peroxide to a solution containing the oxidized halide species under basic conditions. The halide-assisted disproportionation of hydrogen peroxide into water and dioxygen are given in Eqs. (6) and (7). Here, the halogenation of the solvent or ligands has not been detected.



In the presence of sufficient equivalents of H<sub>2</sub>O<sub>2</sub>, substrate and acid each of these complexes has been found to catalyze the bromination of salicylaldehyde giving multiple turnovers in hours at room temperature.

The addition of 2 or more equivalents of HClO<sub>4</sub> to an acetonitrile solution of the complex **1** produced observable changes in the UV/visible spectra with a shift in λ<sub>max</sub> from 685 nm to 765 nm (Fig. 5a) (for complex **2**, a shift in λ<sub>max</sub> occurs from 600 nm to 765 nm, see Fig. 5b) and may be attributed to the formation of [L<sup>i</sup>V-OH]<sup>2+</sup>. In contrast, the addition of 10 equivalent of *tert*-butylammonium bromide in the absence of acid produced no observable change in the UV/visible spectra of these complexes.

The failure to oxidize Br<sup>-</sup> by **1** in the absence of H<sup>+</sup> clearly confirms acid catalyzed oxidation of Br<sup>-</sup>. It was observed that the rate of reaction increases with the increase in [H<sup>+</sup>]. Kinetics were followed under pseudo-first-order conditions taking complex as a minor component and monitoring the change in absorbance of

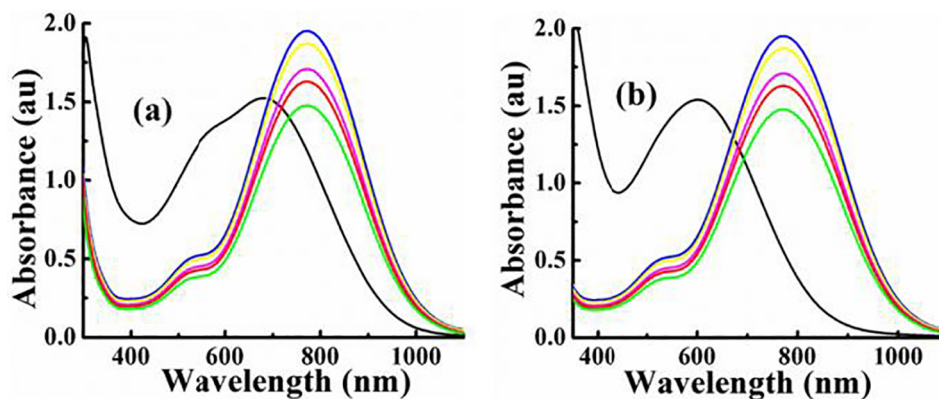


Fig. 5. Shift in  $\lambda_{\text{max}}$  of complex 1 and 2 with addition of  $\text{HClO}_4$  (blue line with 1 equiv acid, yellow with 2 equiv acid, magenta with 4 equiv acid, red with 6 equiv acid and green with 10 equiv acid). (For interpretation of the references to colour in this figure legend, the reader is referred to the web version of this article.)

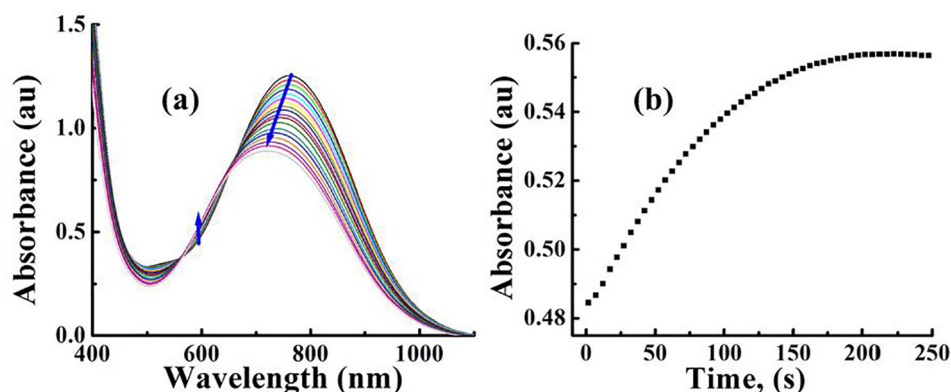


Fig. 6. (a) Time resolved spectra for the catalytic bromination of salicylaldehyde at  $[\text{L}^2(\text{O})\text{VOV}(\text{O})\text{L}^2]$  (complex 2) =  $1 \times 10^{-4}$  M,  $[\text{Substrate}] = 2.5 \times 10^{-3}$  M,  $[\text{Br}^-] = 1.25 \times 10^{-3}$  M and  $[\text{H}_2\text{O}_2] = 1.25 \times 10^{-3}$  M showing two clean isosbestic points at 560 and 650 nm; (b) corresponding kinetic trace at 600 nm.

the complex at either 685 nm (growth curve) or at 765 nm (decay curve) for complex 1 but at both these wavelengths the rate constants evaluated are to be almost identical. The dependence of reaction rates on  $[\text{Br}^-]$  (1.0–10 mM) was carried out keeping  $[\text{I}] = 1.0 \times 10^{-4}$  M,  $[\text{H}^+] = 1.25 \times 10^{-3}$  M and temperature at 25 °C.

From the nature of kinetic traces it is obvious that the reaction is first-order dependent on complex concentration (Figs. 6 and S10 for complex 1). The kinetic studies were carried out at fixed concentration of acid and bromide ion but varying the complex concentration. At each complex concentration we have deduced the

observed rate constant ( $k_{\text{obs}}$ ). Now a plot of  $\log(k_{\text{obs}})$  vs.  $\log[\text{complex}]$  yielded a straight line with slope value 0.925 which clearly manifests a first-order dependence of rate on complex concentration (Fig. S11). A linear least square fit to a plot of  $k_{\text{obs}}$  ( $\text{s}^{-1}$ ) vs.  $[\text{Br}^-]$  yields slope =  $k^{\text{Br}} = 8.82 \pm 0.35$  and  $6.74 \pm 0.19 \text{ M}^{-1}\text{s}^{-1}$  for complex 1 and 2 respectively (Fig. 7).

Analogously, the dependence of rate on  $[\text{H}^+]$  was studied keeping  $[\text{Br}^-] = 1.25 \times 10^{-3}$  M and other conditions remaining the same. A plot of  $k$  ( $=k_{\text{obs}}/[\text{Br}^-]$ ) vs.  $[\text{H}^+]$  gives a non-linear curve of decreasing slope (Fig. 8). Non-linear curve-fitting of experimental

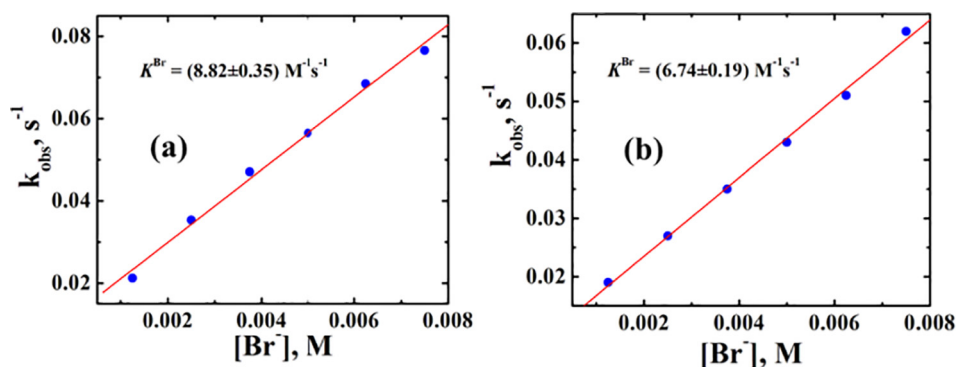
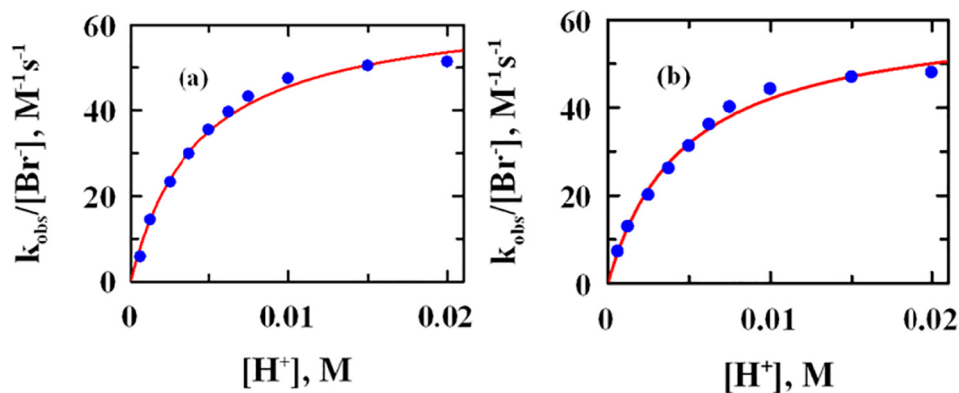


Fig. 7. Variation of rate ( $k_{\text{obs}}$ ) with  $[\text{Br}^-]$  in MeCN at  $[\text{Complex}] = 1 \times 10^{-4}$  M,  $[\text{Substrate}] = 2.5 \times 10^{-3}$  M,  $[\text{H}^+] = 1.25 \times 10^{-3}$  M and  $[\text{H}_2\text{O}_2] = 1.25 \times 10^{-3}$  M for complex 1 (a) and 2 (b).



**Fig. 8.** Variation of  $k_{\text{obs}}/[\text{Br}^-]$  with  $[\text{H}^+]$  in MeCN at  $[\text{Complex}] = 1 \times 10^{-4}$  M,  $[\text{Substrate}] = 2.5 \times 10^{-3}$  M,  $[\text{Br}^-] = 1.25 \times 10^{-3}$  M and  $[\text{H}_2\text{O}_2] = 1.25 \times 10^{-3}$  M for complex **1** (a) and **2** (b).

data to Eq. (11) gives  $K_a = (4.3 \pm 0.40) \times 10^{-3}$  and  $(4.7 \pm 0.50) \times 10^{-3}$  for complex **1** and **2** and  $k^{\text{H}} = (65.0 \pm 2.23)$  and  $(61.87 \pm 2.27) \text{ M}^{-1} \text{ s}^{-1}$  for complex **1** and **2** respectively.

A plausible reaction sequence consistent with the experimental observation may be framed as:

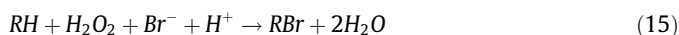
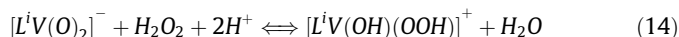
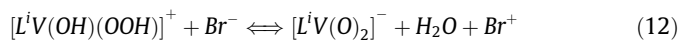


$$\text{rate} = k[\text{VH}][\text{Br}^-] \quad (10)$$

$$k_{\text{obs}} = \frac{k[\text{H}^+][\text{Br}^-]}{K_a + [\text{H}^+]} \quad (11)$$

The very high  $K_a$  is different from  $K_a$  value determined by Pecoraro et al., which corresponds to the protonation of peroxido oxygen atom. In the present reaction this protonation occurs at V = O oxygen atom which might be responsible for significantly higher  $K_a$  values than that reported by Pecoraro et al. [5].

In the presence of multiple equivalents of  $\text{H}_2\text{O}_2$ , bromide and  $\text{H}^+$  ions the vanadium complexes act as catalyst for the peroxidative halogenation of salicylaldehyde. Under this catalytic conditions ( $\text{H}_2\text{O}_2/\text{KBr}$  500 equivalent each with respect to catalyst in mixed solvents  $\text{H}_2\text{O}:\text{MeOH}:\text{THF} = 4:3:2$  in the presence of 2 or more equivalents of  $\text{HClO}_4$  with respect to complex at room temperature) bromination of salicylaldehyde occurs within 12 h with TON 405 and 450 for complexes **1** and **2**, respectively. The catalytic bromination of salicylaldehyde can be rationalized by adopting the following reaction sequences:



To gain some insight into the mechanism of catalytic process, the ground state geometry of complex **2** and some probable catalytic intermediates of **2** ( $2\text{a}^+$ ,  $2\text{b}^+$ ,  $2\text{c}$  and  $2\text{d}^-$ ) formed during the oxidative bromination of salicylaldehyde (Schemes 3 and 5) were performed in the gas phase.

The HOMO–LUMO energy difference is 2.69 eV for the complex **2** which reduces to 2.43 eV for  $2\text{a}^+$ , 3.17 eV for  $2\text{b}^+$  and ultimately 2.85 eV for  $2\text{c}$  giving rise to a species produced by binding of **2** with  $\text{H}_2\text{O}_2$  in acidic medium. The other selected HOMO and LUMO plots of **2** and other intermediates viz.  $2\text{a}^+$ ,  $2\text{b}^+$ ,  $2\text{c}$  and  $2\text{d}^-$  are given into the Figs. S12, S13 and S14.

In case of mono-anionic species,  $2\text{d}^-$  the HOMO–LUMO energy difference is 4.39 eV (Scheme 5), which indicates a more reactive nature of it to form the starting species  $2\text{b}^+$  in the catalytic cycle. So, on the basis of DFT calculation, one can easily frame a catalytic cycle (Scheme 5) which describes the driving force of the catalytic efficiency of **2**. In acidic medium complex **2** ( $[\text{VO}(\text{L}^2)]_2\text{O}$ ) takes up two protons to give  $[\text{L}^2\text{V} = \text{O}]^+$  ( $2\text{a}^+$ ) and  $\text{H}_2\text{O}$ .  $[\text{L}^2\text{V} = \text{O}]^+$  ( $2\text{a}^+$ ) is in protic equilibrium  $[\text{L}^i\text{V} = \text{O}]^+ + \text{H}^+ \rightleftharpoons [\text{L}^i\text{V} = \text{OH}]^{2+}$  ( $2\text{a}^{++}$ ) and is favoured by 420 kcal/mol energy.  $2\text{a}^{++}$  in subsequent step reacts with  $\text{H}_2\text{O}_2$  to give  $[\text{L}^2\text{V}(\text{OH})(\text{OOH})]^+$  ( $2\text{b}^+$ ) which is favoured by 219.4 kcal/mol which then forms **2c** which is favoured by 12.54 kcal/mol (Scheme 3). Now  $2\text{b}^+$  forms  $2\text{d}^-$  through two transient intermediates ( $2\text{b}^{v+}$  and  $2\text{b}^{w+}$ ) where oxidation of  $\text{Br}^-$  to  $\text{Br}^+$  takes place which is favoured by 81.5 kcal/mol.  $2\text{b}^+$  is one of the member of catalytic cycle. Now the regeneration of  $2\text{b}^+$  from  $2\text{d}^-$  is again favoured by  $\sim 338.6$  kcal/mol. So our proposed catalytic Scheme seems to be well suited on the basis of energy consideration obtained from DFT calculations (Table S2).

The existence of  $[\text{L}^2\text{V}(\text{OH})(\text{OOH})]^+$  ( $2\text{b}^+$ ) species in catalytic solution mixture was confirmed by HRMS studies which appears at 456.0933 ( $[\text{L}^2\text{V}(\text{OH})(\text{OOH})]^+ + \text{H}^+$ ) (Fig. S13). Another intermediate  $[\text{L}^2\text{V}(\text{O}_2)]^-$  ( $2\text{d}^-$ ) appears at 437.0948 when the complex treated with  $\text{H}_2\text{O}_2$  (Fig. S14).

#### 4. Conclusion

Dinuclear oxidovanadium(V) complexes  $[\text{L}^1\text{V}^{\text{VO}}(\mu_2\text{-O})\text{VO}(\text{L}^1)]$  (**1**) and  $[\text{L}^2\text{V}^{\text{VO}}(\mu_2\text{-O})\text{VO}(\text{L}^2)]$  (**2**) of ONNO donor amine-bis(phenolate) ligands ( $\text{H}_2\text{L}^1$  and  $\text{H}_2\text{L}^2$ ) have been synthesized and characterized by single crystal X-ray diffraction studies. The complexes **1** and **2** are efficient to catalyze the oxidative bromination of salicylaldehyde in the presence of  $\text{H}_2\text{O}_2$  to produce 5-bromo salicylaldehyde as the major product with TONs more than 400. The kinetic analysis of the bromide oxidation reaction indicates a mechanism which is first order in protonated peroxidovanadium complex and bromide ion and limiting first-order on  $[\text{H}^+]$ . The  $K_a$  of protonated oxido species are:  $K_a = (4.3 \pm 0.40) \times 10^{-3}$  ( $\text{p}K_a = 2.37$ ) and  $(4.7 \pm 0.50) \times 10^{-3}$  ( $\text{p}K_a = 2.33$ ) respectively for complex **1** and **2**. On basis of the chemistry observed for these model compounds, a mechanism of halide oxidation and a detailed catalytic cycle are proposed for the vanadium haloperoxidase enzyme and substantiated by DFT calculations.

#### Acknowledgement

M. Ali thanks to DST West Bengal (Ref. No. 809(Sanc/ST/P/S&T/4G-9/2014) for financial support.

## Appendix A. Supplementary material

Supplementary data associated with this article can be found, in the online version, at <http://dx.doi.org/10.1016/j.ica.2018.04.044>.

## References

- [1] M.R. Maurya, *Coord. Chem. Rev.* 237 (2003) 163.
- [2] (a) A. Butler, *Coord. Chem. Rev.* 187 (1999) 17;  
(b) A. Butler, in: Reedijk, J., Bouwman, E., Dekker, M., (eds.), *Bioinorganic Catalysis*, 2nd ed., New York, 1999 (chapter 5).
- [3] M. Weyand, H.J. Hecht, M. Kieb, M.F. Liaud, H. Vilter, D. Schomburg, *J. Mol. Biol.* 293 (1999) 595.
- [4] M.I. Isupov, A.R. Dalby, A.A. Brindley, Y. Izumi, T. Tanabe, G.N. Murshudov, J.A. Littlechild, *J. Mol. Biol.* 299 (2000) 1035.
- [5] G.J. Colpas, B.J. Hamstra, J.W. Kampf, V.L. Pecoraro, *J. Am. Chem. Soc.* 118 (1996) 3469.
- [6] B.J. Hamstra, G.J. Colpas, V.L. Pecoraro, *Inorg. Chem.* 37 (1998) 949.
- [7] J.A. Littlechild, E. Garcia-Rodriguez, *Coord. Chem. Rev.* 237 (2003) 65.
- [8] S. Macedo-Ribeiro, W. Hemrika, R. Renirie, R. Wever, A. Messerschmidt, *J. Biol. Inorg. Chem.* 209 (1999) 209.
- [9] A. Messerschmidt, R. Wever, *Proc. Natl. Acad. Sci. U.S.A.* 93 (1996) 392.
- [10] P.M. Geschwend, J.K. MacFarlane, K.A. Newman, *Science* 227 (1985) 1033.
- [11] G.W. Gribble, *Chem. Soc. Rev.* 28 (1999) 335.
- [12] A. Butler, in: Reedijk, J., Bouwman, E., Dekker M., (eds.) *Bioinorganic Catalysis*, 2nd ed., New York, 1999, pp. 55–77.
- [13] V.L. Pecoraro, C. Slebodnick, B. Hamstra, in: Crans, D.C., Tracy, A.S. (Ed.), *Vanadium Compounds: Chemistry, Biochemistry and Therapeutic Applications*, ACS Symposium Series, 1998, pp. 711 (chapter 12).
- [14] A. Butler, *Coord. Chem. Rev.* 187 (1999) 17.
- [15] V. Conte, O. Bortolini, M. Carraro, S. Moro, *J. Inorg. Biochem.* 80 (2000) 41.
- [16] O. Bortolini, M. Carraro, V. Conte, S. Moro, *Eur. J. Inorg. Chem.* 1 (2003) 42.
- [17] M. Cásny, D. Rehder, H. Schmidt, V. Conte Vilter, *J. Inorg. Biochem.* 80 (2000) 157.
- [18] R. De La Rose, M.J. Clague, A. Butler, *J. Am. Chem. Soc.* 114 (1992) 760.
- [19] F. Secco, *Inorg. Chem.* 19 (1980) 2722.
- [20] (a) M.J. Clague, N.L. Keder, A. Butler, *Inorg. Chem.* 32 (1993) 4754;  
(b) R. Wever, E. de Boer, B.E. Krenn, H. Offenber, H. Plat, *Prog. Clin. Biol. Res.* 274 (1988) 477;  
(c) R. Wever, W. Hemrika, in: *Vanadium in the Environment. Part 1: Chemistry and Biochemistry*, Wiley, New York, 1997, p. 285.
- [21] D. Maity, A. Ray, W.S. Sheldrick, H.M. Figge, B. Bandyopadhyay, M. Ali, *Inorg. Chim. Acta* 359 (2006) 3197.
- [22] D. Maity, J. Marek, W.S. Sheldrick, H. Mayer-Figge, M. Ali, *J. Mol. Catal. A Chem.* 270 (2007) 153.
- [23] D. Maity, M. Mijanuddin, M.G.B. Drew, J. Marek, P.C. Mondal, B. Pahari, M. Ali, *Polyhedron* 26 (2007) 4494.
- [24] M. Debnath, A. Dutta, S. Biswas, K.K. Das, H.M. Lee, J. Vicha, R. Marek, J. Marek, M. Ali, *Polyherdron* 63 (2013) 189.
- [25] E.Y. Tshuva, I. Goldberg, M. Kol, *Organometallics* 20 (2001) 3017.
- [26] G.M. Sheldrick, *Acta Cryst.* 46 (1990) 467.
- [27] G.M. Sheldrick, T.R. Schneider, *Methods Enzymol.* 277 (1997) 319.
- [28] M. Nardelli, *Comp. Chem.* 7 (1983) 95.
- [29] B.F. Sels, D.E. De Vos, M. Buntinx, P.A. Jacobs, *J. Catal.* 216 (2003) 288.
- [30] R. G. Parr, W. Yang, Oxford University Press, Oxford, 1989.
- [31] (a) T. Liu, H.-X. Zhang, B.-H. Xia, *J. Phys. Chem. A* 111 (2007) 8724;  
(b) X. Zhou, H.-X. Zhang, Q.-J. Pan, B.-H. Xia, A.-C. Tang, *J. Phys. Chem. A* 109 (2005) 8809;  
(c) X. Zhou, A.-M. Ren, J.-K. Feng, *J. Organomet. Chem.* 690 (2005) 338.
- [32] A.D. Becke, *J. Chem. Phys.* 98 (1993) 5648.
- [33] C. Lee, W. Yang, R.G. Parr, *Phys. Rev. B* 37 (1988) 785.
- [34] M. Mahroof-Tahir, A.D. Keramidis, R.B. Goldfrab, O.P. Anderson, M.M. Miller, D.B. Crans, *Inorg. Chem.* 36 (1997) 1657.
- [35] (a) K.K. Rajak, B. Baruah, S.P. Rath, A. Chakravorty, *Inorg. Chem.* 39 (2000) 1598;  
(b) K.K. Rajak, S.P. Rath, S. Mondal, A. Chakravorty, *Inorg. Chem.* 38 (1999) 3283.
- [36] (a) T.K. Paine, T. Weyhermüller, E. Bill, E. Bothe, P. Chaudhuri, *Eur. J. Inorg. Chem.* 24 (2003) 4299;  
(b) G. Asgedom, A. Sreedhara, C.P. Rao, *Polyhedron* 14 (1995) 1873;  
(c) G. Asgedom, A. Sreedhara, J. Kivikoski, J. Valkonen, E. Kolehmainen, C.P. Rao, *Inorg. Chem.* 35 (1996) 5674.
- [37] J.A. Martinez-Perez, M.A. Pickel, E. Caroff, W.-D. Woggon, *Synlett.* 12 (1999) 1875.
- [38] C.L. Perrin, T.J. Dwyer, *Chem. Rev.* 90 (1990) 935.
- [39] A.G.J. Ligtenberg, R. Hage, B.L. Feringa, *Coord. Chem. Rev.* 237 (2003) 89.